



1 **SYNERGY BETWEEN SATELLITE OBSERVATIONS OF SOIL MOISTURE**
2 **AND WATER STORAGE ANOMALIES FOR GLOBAL RUNOFF**
3 **ESTIMATION**

4 Stefania Camici ⁽¹⁾, Gabriele Giuliani ⁽¹⁾, Luca Brocca ⁽¹⁾, Christian Massari ⁽¹⁾, Angelica Tarpanelli
5 ⁽¹⁾, Hassan Hashemi Farahani ⁽²⁾, Nico Sneeuw ⁽²⁾, Marco Restano ⁽³⁾, Jérôme Benveniste ⁽⁴⁾

6 *(1) National Research Council, Research Institute for Geo-Hydrological Protection, Perugia, Italy (s.camici@irpi.cnr.it)*

7 *(2) Institute of Geodesy, University of Stuttgart, Geschwister-Scholl-Straße 24D, 70174 Stuttgart, Germany*

8 *(3) SERCO c/o ESA-ESRIN, Largo Galileo Galilei, Frascati, 00044, Italy*

9 *(4) European Space Agency, ESA-ESRIN, Largo Galileo Galilei, Frascati, 00044, Italy*

10
11
12
13
14
15
16
17
18
19
20
21

* Correspondence to: Ph.D. Stefania Camici, Research Institute for Geo-Hydrological Protection, National Research Council, Via della Madonna Alta 126, 06128 Perugia, Italy. Tel: +39 0755014419
Fax: +39 0755014420 E-mail: stefania.camici@irpi.cnr.it.



22 **ABSTRACT**

23 This paper presents an innovative approach, STREAM - SaTellite based Runoff Evaluation And
24 Mapping - to derive daily river discharge and runoff estimates from satellite soil moisture,
25 precipitation and terrestrial water storage anomalies observations. Within a very simple model
26 structure, the first two variables (precipitation and soil moisture) are used to estimate the quick-flow
27 river discharge component while the terrestrial water storage anomalies are used for obtaining its
28 complementary part, i.e., the slow-flow river discharge component. The two are then summed up to
29 obtain river discharge and runoff estimates.

30 The method is tested over the Mississippi river basin for the period 2003-2016 by using Tropical
31 Rainfall Measuring Mission (TRMM) Multi-satellite Precipitation Analysis (TMPA) rainfall data,
32 European Space Agency Climate Change Initiative (ESA CCI) soil moisture data and Gravity
33 Recovery and Climate Experiment (GRACE) terrestrial water storage data. Despite the model
34 simplicity, relatively high-performance scores are obtained in river discharge simulations, with a
35 Kling-Gupta efficiency index greater than 0.65 both at the outlet and over several inner stations used
36 for model calibration highlighting the high information content of satellite observations on surface
37 processes. Potentially useful for multiple operational and scientific applications (from flood warning
38 systems to the understanding of water cycle), the added-value of the STREAM approach is twofold:
39 1) a simple modelling framework, potentially suitable for global runoff monitoring, at daily time scale
40 when forced with satellite observations only, 2) increased knowledge on the natural processes, human
41 activities and on their interactions on the land.

42

43 Key words: satellite products, soil moisture, water storage variations, data-driven hydrological
44 modelling, rainfall-runoff modelling, Mississippi.



45 **1. INTRODUCTION**

46 Spatial and temporal continuous river discharge monitoring is paramount for improving the
47 understanding of the hydrological cycle, for planning human activities related to water use as well as
48 to prevent/mitigate the losses due to extreme flood events. To accomplish these tasks, runoff and river
49 discharge data, which represents the aggregated signal of runoff (Fekete et al., 2012), should be
50 available at adequate spatial/temporal resolution, i.e., at basin scale (basin area larger than 10⁷000
51 km²) and at monthly time step for water resources management and drought monitoring up to grid
52 scale (few km)/(sub-) daily time step for flood prediction. The accurate continuous (in space and
53 time) runoff and river discharge estimation at finer spatial/temporal resolution is still a big challenge
54 for hydrologists.

55 Traditional in situ observations of river discharge, even if generally characterized by high temporal
56 resolution (up to sub-hourly time step), typically offer little information on the spatial distribution of
57 runoff within a watershed. Moreover, river discharge observation networks suffer from many
58 limitations such as low station density and often incomplete temporal coverage, substantial delay in
59 data access and large decline in monitoring capacity (Vörösmarty et al. 2002). Paradoxically, this
60 latter issue is exacerbated in developing nations (Crochemore et al, 2020), where the knowledge of
61 the terrestrial water dynamics deserves greater attention due to huge damages to settlements and
62 especially the loss of human lives that occurs regularly.

63 This precarious situation has led to growing interest in finding alternative solutions, i.e., model-based
64 or observation-based approaches, for runoff and river discharge monitoring. Model-based
65 approaches, based on the mathematical description of the main hydrological processes (e.g., water
66 balance models, WBMs, global hydrological models, GHMs, e.g., Döll et al., 2003 or, increasing in
67 complexity, land surface models, LSM, e.g., Balsamo et al., 2009; Schellekens et al., 2017), are able
68 to provide comprehensive information on a large number of relevant variables of the hydrological
69 cycle including runoff and river discharge at very high temporal and spatial resolution (up to hourly



70 sampling and 0.05° grid scale). However, the values of simulated water balance components rely on
71 a massive parameterization of the soil, vegetation and land parameters, which is not always realistic,
72 and are strongly dependent on the GHM/ LSM models used, analysis periods (Wisser et al., 2010)
73 and climate forcings selected (e.g Haddeland et al., 2012; Gudmundsson et al., 2012a, b; Prudhomme
74 et al., 2014; Müller Schmied et al., 2016).

75 Alternatively, the observation-based approaches exploit machine learning techniques and a
76 considerable amount of data to describe the physics of the system (i.e. hydraulic and/or hydrologic
77 phenomena, Solomatine and Ostfeld, 2008) with only a limited number of assumptions. Besides being
78 simpler than model-based approaches, these approaches still present some limitations. At first, as they
79 rely on a considerable amount of data describing the modelled system's physics, the spatial/temporal
80 extent and the uncertainty of the resulting dataset is determined by the spatial/temporal coverage and
81 the accuracy of the forcing data (e.g., see E-RUN dataset, Gudmundsson and Seneviratne, 2016;
82 GRUN dataset, Ghiggi et al., 2019; FLO1K dataset, Barbarossa et al., 2018). Additional limitations
83 stem from the employed method to estimate runoff. Indeed, random forests such as employed in
84 Gudmundsson and Seneviratne, 2016, like other machine learning techniques, are powerful tools for
85 data driven modeling, but they are prone to overfitting, implying that noise in the data can obscure
86 possible signals (Hastie et al., 2009). Moreover, the influence of land parameters on continental-scale
87 runoff dynamics is not taken into account as the underlying hypothesis is that the hydrological
88 response of a basin exclusively depend on present and past atmospheric forcing. It is easy to
89 understand that this assumption will only be valid in certain circumstances and might lead to
90 problems, e.g., over complex terrain (Orth and Seneviratne, 2015) or in cases of human river flow
91 regulation (Ghiggi et al., 2019).

92 Remote sensing can provide estimates of nearly all the climate variables of the global hydrological
93 cycle including soil moisture (e.g., Wagner et al., 2007; Seneviratne et al., 2010), precipitation
94 (Huffman et al., 2014) and total terrestrial water storage (e.g., Houborg et al., 2012; Landerer and
95 Swenson, 2012; Famiglietti and Rodell, 2013). It has undeniably changed and improved dramatically



96 the ability to monitor the global water cycle and, hence, runoff. By taking advantage of satellite
97 information, some studies tried to develop methodologies able to optimally produce multivariable
98 datasets from the fusion of in situ and satellite-based observations (e.g., [Rodell et al., 2015](#); [Zhang et](#)
99 [al., 2018](#); [Pellet et al., 2019](#)). Other studies exploited satellite observations of hydrological variables,
100 e.g., precipitation ([Hong et al., 2007](#)), soil moisture ([Massari et al., 2014](#)), and geodetic variables (e.g.,
101 [Sneeuw et al., 2014](#); [Tourian et al., 2018](#)) to monitor single components of the water cycle in an
102 independent way.

103 Although the majority of these studies provide runoff and river discharge data at basin scale and
104 monthly time step, they deserve to be recalled here as important for the purpose of the present study.
105 In particular, [Hong et al. \(2007\)](#) presented a first attempt to obtain an approximate but quasi-global
106 annual streamflow dataset, by incorporating satellite precipitation data in a relatively simple rainfall-
107 runoff simulation approach. Driven by the multiyear (1998-2006) Tropical Rainfall Measuring
108 Mission Multi-satellite Precipitation Analysis, runoff was independently computed for each global
109 land surface grid cell through the Natural Resources Conservation Service (NRCS) runoff curve
110 number (CN) method ([NRCS, 1986](#)) and subsequently routed to the watershed outlet to simulate
111 streamflow. The results, compared to the in situ observed discharge data, demonstrated the potential
112 of using satellite precipitation data for diagnosing river discharge values both at global scale and for
113 medium to large river basins. If, on the one hand, the work of [Hong et al. \(2007\)](#) can be considered
114 as a pioneer study, on the other hand it presents a serious drawback within the NRCS-CN method
115 that lacks a realistic definition of the soil moisture conditions of the catchment before flood events.
116 This aspect is not negligible, as it is well established that soil moisture is paramount in the partitioning
117 of precipitation into surface runoff and infiltration inside a catchment ([Brocca et al., 2008](#)). In
118 particular, for the same rainfall amount but different values of initial soil moisture conditions,
119 different flooding effects can occur (see e.g. [Crow et al., 2005](#); [Brocca et al., 2008](#); [Berthet et al.,](#)
120 [2009](#); [Merz and Blöschl, 2009](#); [Tramblay et al., 2010](#)). On this line following [Brocca et al. \(2009\)](#),
121 [Massari et al. \(2016\)](#) presented a very first attempt to estimate global streamflow data by using



122 satellite Soil Moisture Active and Passive (SMAP) and Global Precipitation Measurement (GPM)
123 products. Although the validation was carried out by routing the monthly surface runoff only in a
124 single basin in Central Italy, the obtained results suggested to dedicate additional efforts in this
125 direction.

126 Among the studies that use satellite observations of hydrological variables for runoff estimation, the
127 hydro-geodetic approaches are undoubtedly worth mentioning, see e.g., ([Sneeuw et al., 2014](#)) for a
128 comprehensive overview or [Lorenz et al. \(2014\)](#) for an analysis of satellite-based water balance
129 misclosures with discharge as closure term. In particular, the satellite mission Gravity Recovery And
130 Climate Experiment (GRACE), which observed the temporal changes in the gravity field, has given
131 a strong impetus to satellite-driven hydrology research ([Tapley et al., 2019](#)). Since temporal gravity
132 field variations over the continents imply water storage change, GRACE was the first remote sensing
133 system to provide observational access to deeper groundwater storage. The relation between GRACE
134 groundwater storage change and runoff was characterized by [Riegger and Tourian \(2014\)](#), which even
135 allowed the quantification of absolute drainable water storage over the Amazon ([Tourian et al., 2018](#)).
136 In essence the storage-runoff relation describes the gravity-driven drainage of a basin and, hence, the
137 slow-flow processes. Due to GRACE's spatial-temporal resolution, runoff and river discharge are
138 generally available for large basins ($>160'000 \text{ km}^2$) and at monthly time step.

139 Based on the above discussion, it is clear that each approach presents strengths and limitations that
140 enable or hamper the runoff and river discharge monitoring at finer spatial and temporal resolutions.
141 In this context, this study presents an attempt to find an alternative method to derive daily river
142 discharge and runoff estimates at $\frac{1}{4}$ degree spatial resolution exploiting satellite observations and the
143 knowledge of the key mechanisms and processes that act in the formation of runoff, i.e., the role of
144 soil moisture in determining the response of a catchment to precipitation. For that, soil moisture,
145 precipitation and terrestrial water storage anomalies (TWSA) observations are used as input into a
146 simple modelling framework named STREAM (SaTellite based Runoff Evaluation And Mapping).
147 Unlike classical land surface models, STREAM exploits the knowledge of the system states (i.e., soil



148 moisture and TWSA) to derive river discharge and runoff, and thus it 1) skips the modelling of the
149 evapotranspiration fluxes which are known to be a non-negligible source of uncertainty (Long et al.
150 2014), 2) limits the uncertainty associated with the over-parameterization of soil and land parameters
151 and 3) implicitly takes into account processes, mainly human-driven (e.g., irrigation, change in the
152 land use), that might have a large impact on the hydrological cycle and hence on runoff.
153 The detailed description of the STREAM model is given in section 4. The collected datasets and the
154 experimental design for the Mississippi River Basin (section 2) are described in sections 3 and 5,
155 respectively. Results, discussion and conclusions are drawn in section 6, 7 and 8, respectively.

156 **2. STUDY AREA**

157 The STREAM model presented here has been tested and validated over the Mississippi River basin.
158 With a drainage area of about 3.3 million km², the Mississippi River basin is the fourth largest
159 watershed in the world, bordered to the West by the crest of the Rocky Mountains and to the East by
160 the crest of the Appalachian Mountains. According to the Köppen climate classification, the climate
161 is subtropical humid over the southern part of the basin, continental humid with hot summer over the
162 central part, continental humid with warm summer over the eastern and norther parts, whereas a
163 semiarid cold climate affects the western part. The average annual air temperature across the
164 watershed ranges from 4°C in the West to 6°C in the East. On average, the watershed receives about
165 900 mm/year of precipitation (77% as rainfall and 23% as snowfall), more concentrated in the eastern
166 and southern portions of the basin with respect to its northern and western part (Vose et al., 2014).
167 The river flow has a clear natural seasonality mainly controlled by spring snowmelt in the
168 mountainous areas of the basins and by heavy rainfall exceeding the soil moisture storage capacity in
169 the central and southern part of the basin (Berghuijs et al., 2016), but it is also heavily regulated by
170 the presence of about 1000 large dams (Global Reservoir and Dam Database GRanD, Lehner et al.,
171 2011) spread-out across the basin. The annual average of Mississippi river discharge at the Vicksburg
172 outlet section is equal to 17'500 m³/s (see Table 1). Given the variety of climate and topography



173 across the Mississippi River basin, it is a good candidate to test the suitability of the STREAM model
174 for river discharge and runoff simulation.

175 3. DATASETS

176 The datasets used in this study include in situ observations, satellite products and model outputs. The
177 first two datasets have been used as input data to the STREAM model. Conversely, the model outputs
178 are used as a benchmark to validate the performance of the STREAM model.

179 3.1 In situ Observations

180 In situ observations comprise air temperature (T_{air}) and river discharge data (Q).
181 For T_{air} data the Climate Prediction Center (CPC) Global Temperature data developed by the
182 American National Oceanic and Atmospheric Administration (NOAA) using the optimal
183 interpolation of quality-controlled gauge records of the Global Telecommunication System (GTS)
184 network (Fan et al., 2008) have been used. The dataset, downloadable at
185 (<https://psl.noaa.gov/data/gridded/data.cpc.globaltemp.html>) is available on a global regular
186 $0.5^\circ \times 0.5^\circ$ grid, and provides daily maximum (T_{max}) and minimum (T_{min}) air temperature data from
187 1979 to present. The daily average air temperature data have been generated as the mean of T_{max} and
188 T_{min} of each day.

189 Daily Q data over the study basins have been taken from the Global Runoff Data Center (GRDC,
190 https://www.bafg.de/GRDC/EN/Home/homepage_node.html). In particular, 11 gauging stations
191 located along the main river network of the Mississippi River basin have been selected to represent
192 the spatial distribution of runoff over the basin. The location of these gauging stations along with
193 relevant characteristics (e.g., the upstream basin area, the mean annual river discharge and the
194 presence of upstream dams) are summarized in Table 1. As it can be noted, mean annual river
195 discharge ranges from 141 to $17\,500 \text{ m}^3/\text{s}$, and 3 out of 11 sections are located downstream big dams
196 (Lehner et al., 2011).



197 **3.2 Satellite Products**

198 Satellite products include observations of precipitation (P), soil moisture and TWSA.

199 The satellite P dataset used in this study is the Multi-satellite Precipitation Analysis 3B42 Version 7
200 (TMPA 3B42 V7) estimate produced by the National Aeronautics and Space Administration (NASA)
201 as the $0.25^\circ \times 0.25^\circ$ quasi-global (50°N-S) gridded dataset. The TMPA 3B42 V7 is a gauged-corrected
202 satellite product, with a latency period of two months after the end of the month of record, available
203 at 3h sampling interval from 1998 to present (2020). Major details about the P dataset, downloadable
204 from <http://pmm.nasa.gov/data-access/downloads/trmm>, can be found in [Huffman et al. \(2007\)](#).

205 Soil moisture data have been taken from the European Space Agency Climate Change Initiative (ESA
206 CCI) Soil Moisture project (<https://esa-soilmoisture-cci.org/>) that provides a product continuously
207 updated in term of spatial-temporal coverage, sensors and retrieval algorithms ([Dorigo et al., 2017](#)).
208 In this study, the daily combined ESA CCI SOIL MOISTURE product v4.2 is used, that is available
209 at global scale with a grid spacing of 0.25° , for the period 1978-2016.

210 TWSA have been obtained from the Gravity Recovery And Climate Experiment (GRACE) satellite
211 mission. Here we employ the NASA Goddard Space Flight Center (GSFC) global mascon model,
212 i.e., Release v02.4, ([Luthcke et al. 2013](#)). It has been produced based on the mass concentration
213 (mascon) approach. The model provides surface mass densities on a monthly basis. Each monthly
214 solution represents the average of surface mass densities within the month, referenced at the middle
215 of the corresponding month. The model has been developed directly from GRACE level-1b K-Band
216 Ranging (KBR) data. It is computed and delivered as surface mass densities per patch over blocks of
217 approximately $1^\circ \times 1^\circ$ or about $12'000 \text{ km}^2$. Although the mascon size is smaller than the inherent
218 spatial resolution of GRACE, the model exhibits a relatively high spatial resolution. This is attributed
219 to a statistically optimal Wiener filtering, which uses signal and noise covariance matrices. The
220 coloured (frequency-dependent) noise characteristic of KBR data was taken in to account when
221 compiling the model, which has allowed for a reliable computation of these noise and signal



222 covariance matrices. They play a crucial role when filtering and allow to achieve a higher spatial
223 resolution compared to commonly applied GRACE filtering methods such as Gaussian smoothing
224 and/or destriping filters. GRACE data are available for the period 01 January 2003 to 15 July 2016.

225 **3.3 Model Outputs**

226 To establish the quality of the STREAM model in runoff simulation, monthly runoff (R) data obtained
227 from the Global Runoff Reconstruction (GRUN_v1, <https://doi.org/10.3929/ethz-b-000324386>) have
228 been used for comparison. The GRUN dataset ([Ghiggi et al., 2019](#)) is a global monthly R dataset
229 derived through the use of a machine learning algorithm trained with in situ Q observations of
230 relatively small catchments (<2500 km²) and gridded precipitation and temperature derived from the
231 Global Soil Wetness Project Phase 3 (GSWP3) dataset, ([Kim et al., 2017](#)). The dataset covers the
232 period from 1902 to 2014 and it is provided on a 0.5° × 0.5° regular grid.

233 **4. METHOD**

234 **4.1 STREAM Model: the Concept**

235 The concept behind the STREAM model is that river discharge is a combination of hydrological
236 responses operating at diverse time scales ([Blöschl et al., 2013](#); [Rakovec et al., 2016](#)). In particular,
237 river discharge can be considered made up of a *slow-flow component*, produced as outflow of the
238 groundwater storage and of a *quick-flow component*, i.e. mainly related to the surface and subsurface
239 runoff components ([Hu and Li, 2018](#)).

240 While the high spatial and temporal (i.e., intermittence) variability of rainfall and the highly changing
241 land cover spatial distribution significantly impact the variability of the *quick-flow component* (with
242 scales ranging from hours to days and meters to kilometres depending on the basin size), *slow-flow*
243 *river discharge* reacts to precipitation inputs more slowly (i.e., months) as water infiltrates, is stored,
244 mixed and is eventually released in times spanning from weeks to months. Therefore, the two
245 components can be estimated by relying upon two different approaches that involve different types



246 of observations. Based on that, within the STREAM model, satellite soil moisture, precipitation and
247 TWSA will be used for deriving river discharge and runoff estimates. The first two variables are used
248 as proxy of the *quick-flow* river discharge component while TWSA is exploited for obtaining its
249 complementary part, i.e., the *slow-flow river discharge* component. Firstly, we exploit the role of the
250 soil moisture in determining the response of the catchment to the precipitation inputs, which have
251 been soundly demonstrated in more than ten years of literature studies (see e.g., [Brocca et al., 2017](#)
252 for a comprehensive discussion on the topic). Secondly, we consider the important role of terrestrial
253 water storage in determining the slow-flow river discharge component as modelled in several
254 hydrological models (e.g., [Sneeuw et al., 2014](#)).

255 It is worth noting that this *modus operandi*, i.e. to model the *quick-flow* and *slow-flow* discharge
256 component separately exploring their process controls independently, has been largely applied and
257 tested in recent and past studies, e.g., for the estimation of the flow duration curve (see e.g., [Botter et](#)
258 [al., 2007a, b](#); [Yokoo and Sivapalan 2011](#); [Muneepeerakul et al., 2010](#); [Ghotbi et al., 2020](#)).

259 **4.2 STREAM Model: the Laws**

260 The STREAM model is a conceptual hydrological model that, by using as input observation of P ,
261 soil moisture, TWSA and T_{air} data, simulates continuous R and Q time series.

262 The model entails three main components (Figure 1): 1) a snow module to separate precipitation into
263 snowfall and rainfall, 2) a soil module to simulate the evolution in time t of the quick and slow runoff
264 responses, Q_{fu} [mm] and Q_{sl} [mm], and 3) a routing module that transfers these components through
265 the basins and the rivers for the simulation of the *quick-flow* river discharge, QF [m^3/s], and the *slow-*
266 *flow* river discharge, SF [m^3/s] components.

267 The soil module is composed of two storages, S_u and S_l as illustrated in Figure 1. The upper storage
268 receives inputs from P , released through a snow module ([Cislaghi et al., 2020](#)) as rainfall (r) or stored
269 as snow water equivalent (SWE) within the snowpack and on the glaciers. In particular, according to



270 Cislaghi et al. (2020), *SWE* is modelled by using as input T_{air} and a degree-day coefficient, C_m , to be
271 estimated by calibration.

272 Once separated, r input contributes to the quick runoff response while the *SWE* (like other fluxes
273 contributing to modify the soil water content into Su) is neglected as already considered in the satellite
274 TWSA. Therefore, the first key point of the STREAM model is that the water content in the upper
275 storage is directly provided by the satellite soil moisture observations and the loss processes like
276 infiltration or evaporation do not need to be explicitly modelled to simulate the evolution in time t of
277 soil moisture. Consequently, the quick runoff response, Qfu from the first storage can be computed
278 through equation (1) as follows:

$$279 \quad Qfu(t) = r(t) SWI(t, T)^\alpha \quad (1)$$

280 where:

281 - *SWI* is the Soil Water Index (Wagner et al., 1999), i.e., the root-zone soil moisture product referred
282 to the first layer of the model, derived by the surface satellite soil moisture product, θ , by applying
283 the exponential filtering approach in its recursive formulation (Albergel et al., 2009):

$$284 \quad SWI_n = SWI_{n-1} + K_n(\theta(t_n) - SWI_{n-1}) \quad (2)$$

285 with the gain K_n at the time t_n given by:

$$286 \quad K_n = \frac{K_{n-1}}{K_{n-1} + e^{\left(\frac{t_n - t_{n-1}}{T}\right)}} \quad (3)$$

287 - T [days] is a parameter, named characteristic time length, that characterizes the temporal variation
288 of soil moisture within the root-zone profile and the gain K_n ranges between 0 and 1;

289 - α [-] is a coefficient linked to the non-linearity of the infiltration process and it takes into account
290 the characteristics of the soil;

291 - for the initialization of the filter $K_1 = 1$ and $SWI_1 = \theta(t_1)$.



292 The second key point of STREAM approach concerns the estimation of the slow runoff response, Q_{sl} ,
293 from the second storage. The hypothesis here, shared also with other studies (e.g., [Rakovec et al., 2016](#)),
294 is that the dynamic of the slow runoff component can be represented by the monthly TWSA data.
295 Indeed, the time scale of slow runoff response is typically in the range of seasons to years and it is
296 almost independent upon the water that is contained in that upper storage. For that, the slow runoff
297 response Q_{sl} , from the second storage, can be computed through equation (4) as follows:

$$298 \quad Q_{sl}(t) = \beta (TWSA^*(t))^m \quad (4)$$

299 where:

300 - $TWSA^*$ [-] is the TWSA estimated by GRACE normalized by its minimum and maximum values.

301 The assumption behind this equation is that TWSA can be assumed as a proxy of the evolution in
302 time, t , of the Sl , i.e., the storage of the lower storage.

303 - β [mm h^{-1}] and m [-] are two parameters describing the nonlinearity between slow runoff
304 component and $TWSA^*$.

305 Note that, being based on a conceptual framework, we assume that soil moisture acts both on the
306 generation of the quick flow part (mainly) and is partly responsible of the slow flow contribution
307 indirectly via TWSA observations (indeed TWSA already contains the soil moisture signal in
308 themselves).

309 The STREAM model runs in a semi-distributed version in which the catchment is divided into s
310 elements, each one representing either a subcatchment with outlet along the main channel or an area
311 draining directly into the main channel. Each element is assumed homogeneous and hence constitutes
312 a lumped system.

313 The routing module (controlled by a γ parameter) conveys the Q_{fu} and Q_{sl} response components at
314 each element outlet (subcatchments and directly draining areas, [Brocca et al., 2011](#)) and successively
315 at the catchment outlet of the basin. Specifically, the quick component Q_{fu} is routed to the element



316 outlet by the Geomorphological Instantaneous Unit Hydro-graph (GIUH, Gupta et al., 1980) for
317 subcatchments or through a linear reservoir approach (Nash, 1957) for directly draining areas; the
318 Qsl slow component is transferred to the outlet section by a linear reservoir approach. Finally, a
319 diffusive linear approach (controlled by the parameters C and D , i.e., Celerity and Diffusivity,
320 Troutman and Karlinger, 1985) is applied to route the quick and slow runoff components at the outlet
321 section of the catchment (Brocca et al., 2011). In the first case we obtain the *quick-flow* river discharge
322 component, QF [m^3/s], and in the second case the *slow-flow* river discharge component, SF [m^3/s]
323 (see Figure 1).

324 **4.3 STREAM Parameters**

325 The STREAM model uses 8 parameters of which 5 are used in the soil module (α , T [days], β [mm
326 h^{-1}], m , C_m) and 3 in the routing module (γ , C [$km\ h^{-1}$] and D [$km^2\ h^{-1}$]). These parameters are
327 calibrated by maximizing the Kling-Gupta Efficiency index (KGE, Gupta et al., 2009; Kling et al.,
328 2012, see paragraph 5.1 for more details) between observed and simulated river discharge.

329 **5. EXPERIMENTAL DESIGN**

330 **5.1 Modelling Setup for Mississippi River Basin**

331 The modelling setup is carried out in four steps (Figure 2):

332 1. *Input data collection*. Two different groups of data have to be collected to setup the model, i.e.,
333 topographic information and hydrological variables. Concerning the topographic information, the
334 SHuttle Elevation Derivatives at multiple Scales (HydroSHED, <https://www.hydrosheds.org/>) DEM
335 of the basin at the $3''$ resolution (nearly 90 m at the equator) as well as the location of the gauging
336 stations where the model should be calibrated/validated, are collected. Concerning the hydrological
337 variables, gridded precipitation, T_{air} , soil moisture and TWSA are collected. In addition, in situ Q
338 time series for the sections where the model should be calibrated/validated as well as modelled runoff
339 datasets are required.



340 2. *Sub-basin delineation*. STREAM model is run in the semi-distributed version over the Mississippi
341 River basin. The TopoToolbox (<https://topotoolbox.wordpress.com/>), a tool developed in Matlab by
342 Schwanghart et al. (2010), and the DEM of the basin have been used to derive flow directions, to
343 extract the stream network and to delineate the drainage basins over the Mississippi River basin. In
344 particular, by considering only rivers with Horton-Strahler order greater than 3, the Mississippi
345 watershed has been divided into 53 sub-basins as illustrated in Figure 3. Red dots in the figure indicate
346 the location of the 11 discharge gauging stations selected for the study area.

347 3. *Extraction of input data*. Precipitation, T_{air} , soil moisture and TWSA datasets data have to be
348 extracted for each sub-basin of the study area. If characterized by different spatial resolution, these
349 datasets need to be resampled over a common spatial grid prior to be used as input into the model.
350 To run the STREAM model over the Mississippi river basin, input data have been resampled over the
351 precipitation spatial grid at 0.25° resolution through a bilinear interpolation. For each of the 53
352 Mississippi subbasins, the resampled precipitation, soil moisture, T_{air} and TWSA data have been
353 extracted.

354 4. *STREAM model calibration*. In situ river discharge data are used as reference data for the
355 calibration of STREAM model. For Mississippi, the STREAM model has been calibrated over five
356 sections as illustrated in Figure 3: the inner sections 4, 6, 9, 11 and the outlet section 10, are used to
357 calibrate the model and all sub-basins contributing to the respective sections are highlighted with the
358 same colour. This means that, for example, the sub-basins labelled as 1, 2, 5 to 15, 17, 22, 23, and 30
359 contribute to section 4, sub-basins 31, 37, 38 and 41 contribute to section 6 and so on. Consequently,
360 the sub-basins highlighted with the same colour are assigned the same model parameters, i.e. the
361 parameters that allow to reproduce the river discharge data observed at the related outlet section.

362 Once calibrated, the STREAM model has been run to provide continuous daily Q and R time series,
363 at the outlet section of each subbasin and over each grid pixel, respectively. By considering the
364 spatial/temporal availability of both in situ and satellite observations, the entire analysis period covers
365 the maximum common observation period, i.e., from 01 January 2003 to 15 July 2016 at daily time



366 scale. To establish the goodness-of-fit of the model, the simulated river discharge and runoff
367 timeseries are compared against in situ river discharge and modelled runoff data.

368 **5.2 Model Evaluation Criteria and Performance Metrics**

369 The model has been run over a 13.5-year period split into two sub periods: the first 8 years, from
370 January 2003 to December 2010, have been used to calibrate the model successively validated over
371 the remaining 5.5 years (January 2011 - July 2016).

372 In particular, three different validation schemes have been adopted to assess the robustness of the
373 STREAM model:

- 374 1. Internal validation aimed to test the plausibility of both the model structure and the parameter
375 set in providing reliable estimates of the hydrological variables against which the model is
376 calibrated. For this purpose, a comparison between observed and simulated river discharge
377 time series on the sections used for model calibration has been carried out for both the
378 calibration and validation sub periods.
- 379 2. Cross-validation testing the goodness of the model structure and the calibrated model
380 parameters to predict hydrological variables at locations not considered in the calibration
381 phase. In this respect, the cross-validation has been carried out by comparing observed and
382 simulated river discharge time series in gauged basins not considered during the calibration
383 phase;
- 384 3. External validation aimed to test the capability of the model “*to get the right answers for the*
385 *right reasons*” ([Kirchner 2006](#)). In this respect, the capability of the model to reproduce
386 variables (e.g., fluxes or state variables) other than discharge and not considered in the
387 calibration phase, should be tested. As runoff is a secondary product of the STREAM model,
388 obtained indirectly from the calibration of the river discharge (basin-integrated runoff), the
389 comparison in terms of runoff can be considered as a further external validation of the model.
390 Runoff, differently from discharge, cannot be directly measured. It is generally modelled
391 through land surface or hydrological models. Its validation requires a comparison against



392 modelled data that, however, suffer from uncertainties (Beck et al., 2017). Based on that, in
393 this study the GRUN runoff dataset described in the section 3.3 has been used for a qualitative
394 comparison.

395 5.3 Performance Metrics

396 To measure the goodness-of-fit between simulated and observed river discharge data three
397 performance scores have been used:

- 398 • the relative root mean square error, RRMSE:

$$399 \text{ RRMSE} = \frac{\sqrt{\frac{1}{n} \sum_{i=1}^n (Q_{sim_i} - Q_{obs_i})^2}}{\frac{1}{n} \sum_{i=1}^n (Q_{obs_i})} \quad (5)$$

400 where Q_{obs} and Q_{sim} are the observed and simulated discharge time series of length n . RRMSE
401 values range from 0 to $+\infty$, the lower the RRMSE, the better the agreement between observed and
402 simulated data.

- 403 • the Pearson correlation coefficient, R , measures the linear relationship between two variables:

$$404 R = \frac{\sum_{i=1}^n (Q_{sim_i} - \overline{Q_{sim_i}})(Q_{obs_i} - \overline{Q_{obs_i}})}{\sqrt{\sum_{i=1}^n (Q_{sim_i} - \overline{Q_{sim_i}})^2 (Q_{obs_i} - \overline{Q_{obs_i}})^2}} \quad (6)$$

405 where $\overline{Q_{obs}}$ and $\overline{Q_{sim}}$ represent the mean values of Q_{obs} and Q_{sim} , respectively. The values of R range
406 between -1 and 1 ; higher values of R indicate a better agreement between observed and simulated
407 data.

- 408 • the Kling-Gupta efficiency index (KGE, Gupta et al., 2009), which provides direct assessment
409 of four aspects of discharge time series, namely shape, timing, water balance and variability. It
410 is defined as follows:

$$411 \text{ KGE} = 1 - \sqrt{(R - 1)^2 + (\delta - 1)^2 + (\varepsilon - 1)^2} \quad (7)$$

412 where R is the correlation coefficient, δ the relative variability and ε the bias normalized by the
413 standard deviation between observed and simulated discharge. The KGE values range between $-\infty$
414 and 1 ; the higher the KGE, the better the agreement between observed and simulated data.
415 Simulations characterized by values of KGE in the range -0.41 and 1 can be assumed as reliable;



416 values of KGE greater than 0.5 have been assumed good with respect to their ability to reproduce
417 observed time series ([Thiemig et al., 2013](#)).

418 **6. RESULTS**

419 The testing and validation of the STREAM model is presented and discussed in this section according
420 to the scheme illustrated in section 5.2.

421 **6.1 Internal Validation**

422 The performance of the STREAM model over the calibrated river sections is illustrated in Figure 4
423 and summarized in Table 2. Figure 4 shows observed and simulated river discharge time series over
424 the whole study period (2003-2016); in Table 2 the performance scores are evaluated separately for
425 the calibration and validation sub periods. It is worth noting that the model accurately simulates the
426 observed river discharge data and is able to give the “right answer” with good modelling
427 performances. Score values of KGE and R over the calibration (validation) period are higher than
428 0.62 (0.67) and 0.75 (0.75) (resp.) for all the sections; RRMSE is lower than 46% (51%) for all the
429 sections except for section 9, where it rises up to 71% (77%). The performances remain good even if
430 they are evaluated over the entire study period as indicated by the scores on the top of each plot of
431 Figure 4.

432 **6.2 Cross-validation**

433 The cross-validation has been carried out over the six river sections illustrated in Figure 5 not used
434 in the calibration step. The performance scores on the top of each plot refer to the entire study periods;
435 the scores split for calibration and validation periods are reported in Table 2. For some river sections
436 the performance is quite low (see, e.g., river section 1, 2 and 5) whereas for others the model is able
437 to simulate the observed discharge data quite accurately (e.g., 7 and 8). In particular, for river sections
438 1, 2 even if KGE reaches values equal to 0.35 and 0.40 (for the whole period), respectively, there is
439 not a good agreement between observed and simulated river discharge and the R score is lower than
440 0.55 for both river sections. The worst performance is obtained over section 5, with negative KGE



441 and low R (high RRSME). These results are certainly influenced by the presence of dams located
442 upstream to these river sections (see Table 1): the model, not having a specific module for modelling
443 reservoirs, is not able to accurately reproduce the dynamics of river discharge over regulated river
444 sections. Better performances are obtained over river sections 3 (slightly influenced by the presence
445 of dams in section 1 and 2), 7 and 8. In particular, over river section 7, the STREAM model
446 overestimates the observed river discharge highlighting that the model parameters estimated for river
447 section 6 are not suitable to accurately reproduce river discharge for river section 7 (see Figure 3 and
448 Figure 5). Conversely, the performances over river section 8, whose parameters have been set equal
449 to the ones of river section 10, are quite high (KGE equal to 0.71, 0.80 and 0.77 for the entire, the
450 calibration and the validation period, respectively; R equal to 0.83, 0.84 and 0.84 for the entire,
451 calibration and validation periods, respectively).

452 This finding, which could be due to different/similar interbasin characteristics, raises doubts about
453 the robustness of model parameters and whether it is actually possible to transfer model parameters
454 from one river section to another. A more in-depth investigation about the model calibration
455 procedure will be carried out in future studies.

456 **6.3 External Validation**

457 For the external validation, the monthly runoff time series provided by the GRUN datasets have been
458 compared against the ones computed by the STREAM model. For that, STREAM daily runoff time
459 series have been aggregated at monthly scale and re-gridded at the same spatial resolution of the
460 GRUN dataset (0.5°). The comparison is illustrated in Figure 6 for the common period 2003–2014.
461 Although the two datasets consider different rainfall inputs, the two models agree in identifying two
462 distinct zones, i.e., the western and the eastern area. Likely due to the calibration procedure, the
463 STREAM runoff map appears patchier with respect to GRUN and discontinuities along the sub-basin
464 boundaries (identified in Figure 3) can be noted. This should be ascribed to the automatic calibration
465 procedure of the model that, differently from other calibration techniques (e. g., regionalization
466 procedures), does not consider the basin physical attributes like soil, vegetation, and geological



467 properties that govern spatial dynamics of hydrological processes. This calibration procedure can
468 generate sharp discontinuities even for neighbouring subcatchments individually calibrated. It leads
469 to discontinuities in model parameter values and consequently in the simulated hydrological variable
470 (runoff).

471 7. DISCUSSION

472 In the previous sections, the ability of the STREAM model to accurately simulate river discharge and
473 runoff time series has been presented. In particular, Figures 4, 5 and 6 demonstrate that satellite
474 observations of precipitation, soil moisture and terrestrial water storage anomalies can provide
475 accurate daily river discharge estimates for near-natural large basins (absence of upstream dams), and
476 for basins with draining area lower than $160'000 \text{ km}^2$ (see section 7), i.e., at spatial/temporal
477 resolution lower than the ones of the TWSA input data (monthly, $160'000 \text{ km}^2$). This is an important
478 result of the study as it demonstrates, on one hand, that the model structure is appropriate with respect
479 to the data used as input and, on the other hand, the great value of information contained into TWSA
480 data that, even if characterized by limited spatial/temporal resolution, can be used to simulate runoff
481 and river discharge at basin scale. Hereinafter, the strengths and the main limitations of the STREAM
482 approach are discussed.

483 Among the strengths of the STREAM model it is worth highlighting:

484 1. **Remote sensing-based data-driven model.** Discharge and runoff estimates are obtained through
485 a remote sensing-based data-driven model, simpler than classical hydrological models or LSMs. In
486 particular, discharge and runoff estimates are obtained by exploiting as much as possible satellite
487 observations and by keeping the modelling component at a minimum. The knowledge of the key
488 mechanisms and processes that act in the formation of runoff, like the role of the soil moisture in
489 determining the response of the catchment to precipitation, played a major role in the definition of
490 the model structure. Being an observational-based approach, the STREAM model presents two main
491 advantages: 1) possibility to directly ingest observations (soil moisture and terrestrial water storage



492 data) into the model structure, allowing to take implicitly into account some processes, mainly
493 human-driven (e.g., irrigation, change in the land use), which might have a large impact on the
494 hydrological cycle and hence on total runoff; 2) the independence with respect to existing large scale
495 hydrological models such as, e.g., the evapotranspiration is not explicitly modelled.

496 2. **Simplicity.** The STREAM data-driven structure: 1) limits the input data required (only
497 precipitation, T_{air} , soil moisture and TWSA data are needed as input; LSM/GHMs require many
498 additional inputs such as wind speed, shortwave and longwave radiation, pressure and relative
499 humidity); 2) limits and simplifies the processes to be modelled for runoff/discharge simulation.
500 Processes like evapotranspiration, infiltration or percolation, are not modelled therefore avoiding the
501 need of using sophisticated and highly parameterized equations (e.g., Penman-Monteith for
502 evapotranspiration, [Allen et al., 1998](#), Richard equation for infiltration, [Richard, 1931](#)); 3) limits the
503 number of parameters (only 8 parameters have to be calibrated) thus simplifying the calibration
504 procedure and potentially reduce the model uncertainties related to the estimation of parameter
505 values.

506 3. **Versatility.** The STREAM model is a versatile model suitable for daily runoff and discharge
507 estimation over sub-basins with different physiographic characteristics. The results obtained in this
508 study clearly indicate the potential of this approach to be extended at the global scale. Moreover, the
509 model can be easily adapted to ingest input data with spatial/temporal resolution different from the
510 one tested in this study (0.25°/daily). For instance, satellite missions with higher space/time
511 resolution, or near real time satellite products could be considered. As an example, the Next
512 Generation Gravity Mission design studies all encompass double-pair scenarios, which would greatly
513 improve upon the current spatial resolution of single-pair missions like GRACE and GRACE-FO (>
514 100'000 km²).

515 4. **Computationally inexpensive.** Due to its simplicity and the limited number of parameters to be
516 calibrated, the computational effort for the STREAM model is very limited.



517

518 However, some limitations have to be acknowledged for the current version of the STREAM model:

519 **1. Presence of reservoir, diversion, dams or flood plain.** As the STREAM model does not explicitly
520 consider the presence of discontinuity elements along the river network (e. g, reservoir, dam or
521 floodplain), discharge estimates obtained for sections located downstream of such elements might be
522 inaccurate (see, e.g., river sections 1 and 2 in Figure 5).

523 **2. Need of in situ data for model calibration and robustness of model parameters.** As discussed
524 in the results section, parameter values of the STREAM model are set through an automatic
525 calibration procedure aimed at minimizing the differences between simulated and observed river
526 discharge. The main drawback of this parameterization technique is that the models parameterized
527 with this technique may exhibit (1) poor predictability of state variables and fluxes at locations and
528 periods not considered in the calibration, and (2) sharp discontinuities along sub-basin boundaries in
529 state flux, and parameter fields (e.g., [Merz and Blöschl, 2004](#)).

530 To overcome these issues, several regionalization procedures, as for instance summarized in [Cislaghi](#)
531 [et al. \(2020\)](#), could be conveniently applied to transfer model parameters from hydrologically similar
532 catchments to a catchment of interest. In particular, the regionalization of model parameters could
533 allow to: i) estimate discharge and runoff time series over ungauged basins overcoming the need of
534 discharge data recorded from in-situ networks; ii) estimate the model parameter values through a
535 physically consistent approach, linking them to the characteristics of the basins; iii) solve the problem
536 of discontinuities in the model parameters, avoiding to obtain patchy unrealistic runoff maps.

537 **8. CONCLUSIONS**

538 This study presents a new data-driven model, STREAM, for runoff and river discharge estimation.
539 By using as input satellite data of precipitation, soil moisture and terrestrial water storage anomalies,
540 the model has been able to provide accurate daily river discharge and runoff estimates at the outlet



541 river section and the inner river sections and over a $0.25^{\circ} \times 0.25^{\circ}$ spatial grid of the Mississippi river
542 basin. In particular, the model is suitable to reproduce:

- 543 1. river discharge time series over the calibrated river section with good performances both in
544 calibration and validation periods;
- 545 2. river discharge time series over river sections not used for calibration and not located downstream
546 dams or reservoirs;
- 547 3. runoff time series with a quite good agreement with respect to the well-established GRUN
548 observational-based dataset used for comparison.

549 The integration of observations of soil moisture, precipitation and terrestrial water storage anomalies
550 is a first alternative method for river discharge and runoff estimation with respect to classical methods
551 based on the use of TWSA-only (suitable for river basins larger than $160'000 \text{ km}^2$, monthly time
552 scale) or on classical LSMs (Cai et al., 2014).

553 Moreover, although simple, the model has demonstrated a great potential to be easily applied over
554 subbasins with different climatic and topographic characteristics, suggesting also the possibility to
555 extend its application to other basins. In particular, the analysis over basins with high human impact,
556 where the knowledge of the hydrological cycle and the river discharge monitoring is very important,
557 deserves special attention. Indeed, as the STREAM model is directly ingesting observations of soil
558 moisture and terrestrial water storage data, it allows the modeller to neglect processes that are
559 implicitly accounted for in the input data. Therefore, human-driven processes (e.g., irrigation, land
560 use change), that are typically very difficult to simulate due to missing information and might have a
561 large impact on the hydrological cycle, hence on total runoff, could be implicitly modelled. The
562 application of the STREAM model on a larger number of basins is also required to investigate the
563 possibility to regionalize the model parameters and overcome the limitations of the automatic
564 calibration procedure highlighted in the discussion section.



565 **AUTHOR CONTRIBUTION**

566 S.C. performed the analysis and wrote the manuscript. G.G. collected the data and helped in
567 performing the analysis; C.M, L.B., A.T., N.S., H.H.F., C.M., M.R. and J.B. contributed to the
568 supervision of the work. All authors discussed the results and contributed to the final manuscript.

569 **CODE AVAILABILITY**

570 The STREAM model code will be made available once the manuscript will be published.

571 **DATA AVAILABILITY**

572 All data and codes used in the study are freely available online. Air temperature data are available at
573 <https://psl.noaa.gov/data/gridded/data.cpc.globaltemp.html> (last access 25/11/202). In situ river
574 discharge data have been taken from the Global Runoff Data Center (GRDC,
575 https://www.bafg.de/GRDC/EN/Home/homepage_node.html (last access 25/11/202). Precipitation
576 and soil moisture data are available from <http://pmm.nasa.gov/data-access/downloads/trmm> and
577 <https://esa-soilmoisture-cci.org/>, respectively.

578 **COMPETING INTERESTS**

579 The authors declare that they have no conflict of interest.

580 **ACKNOWLEDGMENTS**

581 The authors wish to thank the Global Runoff Data Centre (GRDC) for providing most of the
582 streamflow data throughout Europe. The authors gratefully acknowledge support from ESA through
583 the STREAM Project (EO Science for Society element Permanent Open Call contract n°
584 4000126745/19/I-NB).

585



586 **REFERENCE**

- 587 Albergel, C., Rüdiger, C., Carrer, D., Calvet, J. C., Fritz, N., Naeimi, V., Bartalis, Z., & Hasenauer, S. (2009). An
588 evaluation of ASCAT surface soil moisture products with in-situ observations in southwestern France. *Hydrology and*
589 *Earth System Sciences*, 13, 115–124, doi:10.5194/hess-13-115-2009.
- 590 Allen RG, Pereira LS, Raes D, Smith M (1998) Crop evapotranspiration — guidelines for computing crop water
591 requirements. FAO Irrigation & Drainage Paper 56. FAO, Rome.
- 592 Balsamo, G., A. Beljaars, K. Scipal, P. Viterbo, B. vanden Hurk, M. Hirschi, and A. K. Betts (2009). A revised hydrology
593 for the ECMWF model: Verification from field site to terrestrial water storage and impact in the integrated forecast
594 system, *J. Hydrometeorol.*, 10(3), 623–643, doi:10.1175/2008JHM1068.1.
- 595 Barbarossa, V., Huijbregts, M. A., Beusen, A. H., Beck, H. E., King, H., & Schipper, A. M. (2018). FLO1K, global maps
596 of mean, maximum and minimum annual streamflow at 1 km resolution from 1960 through 2015. *Scientific data*, 5,
597 180052.
- 598 Beck, H. E., van Dijk, A. I., de Roo, A., Dutra, E., Fink, G., Orth, R., & Schellekens, J. (2017). Global evaluation of
599 runoff from ten state-of-the-art hydrological models. *Hydrology and Earth System Sciences*, 21(6), 2881–2903. doi:
600 doi.org/10.5194/hess-21-2881-2017.
- 601 Berghuijs, W. R., Woods, R. A., Hutton, C. J., and Sivapalan, M. (2016). Dominant flood generating mechanisms across
602 the United States, *Geophys. Res. Lett.*, 43, 4382–4390, <https://doi.org/10.1002/2016GL068070>.
- 603 Berthet, L., Andréassian, V., Perrin, C., & Javelle, P. (2009). How crucial is it to account for the antecedent moisture
604 conditions in flood forecasting? Comparison of event-based and continuous approaches on 178 catchments.
605 *Hydrology and Earth System Sciences*, 13(6), 819–831.
- 606 Blöschl, G., Sivapalan, M., Wagener, T., Viglione, A., & Savenije, H. H. G. (Eds.) (2013). *Runoff predictions in ungauged*
607 *basins: A synthesis across processes, places and scales*. Cambridge: Cambridge University Press.
- 608 Botter, G., Peratoner, F., Porporato, A., Rodriguez-Iturbe, I., and Rinaldo, A. (2007b). Signatures of large-scale soil
609 moisture dynamics on streamflow statistics across U.S. Climate regimes, *Water Resour. Res.*, 43, W11413,
610 doi:10.1029/2007WR006162.
- 611 Botter, G., Porporato, A., Daly, E., Rodriguez-Iturbe, I., and Rinaldo, A. (2007a). Probabilistic characterization of base
612 flows in river basins: Roles of soil, vegetation, and geomorphology, *Water Resour. Res.*, 43,
613 W06404, doi:10.1029/2006WR005397.
- 614 Brocca, L., Melone, F., Moramarco, T. (2008). On the estimation of antecedent wetness conditions in rainfall-runoff
615 modelling. *Hydrological Processes*, 22 (5), 629–642, doi:10.1002/hyp.6629. <http://dx.doi.org/10.1002/hyp.6629>.
- 616 Brocca, L., Melone, F., Moramarco, T., & Morbidelli, R. (2009). Antecedent wetness conditions based on ERS
617 scatterometer data. *Journal of Hydrology*, 364(1–2), 73–87
- 618 Brocca, L., Melone, F., & Moramarco, T. (2011). Distributed rainfall-runoff modelling for flood frequency estimation
619 and flood forecasting. *Hydrological processes*, 25(18), 2801–2813.
- 620 Brocca, L., Ciabatta, L., Massari, C., Camici, S., & Tarpanelli, A. (2017). Soil moisture for hydrological applications:
621 open questions and new opportunities. *Water*, 9(2), 140.
- 622 Cai, X., Yang, Z. L., David, C. H., Niu, G. Y., & Rodell, M. (2014). Hydrological evaluation of the Noah-MP land surface
623 model for the Mississippi River Basin. *Journal of Geophysical Research: Atmospheres*, 119(1), 23–38.
- 624 Cislighi, A., Masseroni, D., Massari, C., Camici, S., & Brocca, L. (2020). Combining a rainfall–runoff model and a
625 regionalization approach for flood and water resource assessment in the western Po Valley, Italy. *Hydrological*
626 *Sciences Journal*, 65(3), 348–370.
- 627 Crochemore, L., Isberg, K., Pimentel, R., Pineda, L., Hasan, A., & Arheimer, B. (2020). Lessons learnt from checking
628 the quality of openly accessible river flow data worldwide. *Hydrological Sciences Journal*, 65(5), 699–711
- 629 Crow, W. T., Bindlish, R., & Jackson, T. J. (2005). The added value of spaceborne passive microwave soil moisture
630 retrievals for forecasting rainfall-runoff partitioning. *Geophysical Research Letters*, 32(18).



- 631 Döll, P., F.Kaspar, and B.Lehner (2003), A global hydrological model for deriving water availability indicators: Model
632 tuning and validation, *J. Hydrol.*, 270(1–2), 105–134, doi:10.1016/S0022-1694(02)00283-4.
- 633 Dorigo, W., Wagner, W., Albergel, C., Albrecht, F., Balsamo, G., Brocca, L., Chung, D., Ertl, M., Forkel, M., Gruber, A.,
634 Haas, D., Hamer, P. Hirschi, M., Ikonen, J., de Jeu, R., Kidd, R., Lahoz, W., Liu, Y.Y., Miralles, D., Mistelbauer, T.,
635 Nicolai-Shaw, N., Parinussa, R., Pratola, C., Reimer, C., van der Schalie, R., Seneviratne, S.I., Smolander, T.,
636 Lecomte, P. (2017). ESA CCI Soil Moisture for improved Earth system understanding: state-of-the art and future
637 directions. *Remote Sensing of Environment*, 203, 185-215.
- 638 Famiglietti, J. S., & Rodell, M. (2013). Water in the balance. *Science*, 340(6138), 1300-1301.
- 639 Fan, Y. & Van den Dool, H. A (2008). Global monthly land surface air temperature analysis for 1948–present. *Journal of*
640 *Geophysical Research: Atmospheres* 113, D01103.
- 641 Fekete, B. M., Looser, U., Pietroniro, A., and Robarts, R. D. (2012). Rationale for monitoring discharge on the ground,
642 *J. Hydrometeorol.*,13, 1977–1986.
- 643 Ghiggi, G., Humphrey, V., Seneviratne, S. I., & Gudmundsson, L. (2019). GRUN: an observation-based global gridded
644 runoff dataset from 1902 to 2014. *Earth System Science Data*, 11(4), 1655-1674.
- 645 Ghotbi, S., Wang, D., Singh, A., Blöschl, G., & Sivapalan, M. (2020). A New Framework for Exploring Process Controls
646 of Flow Duration Curves. *Water Resources Research*, 56(1), e2019WR026083.
- 647 Gudmundsson, L., & Seneviratne, S. I. (2016). Observation-based gridded runoff estimates for Europe (E-RUN version
648 1.1). *Earth System Science Data*, 8(2), 279-295.
- 649 Gudmundsson, L., Wagener, T., Tallaksen, L. M., & Engeland, K. (2012a). Evaluation of nine large-scale hydrological
650 models with respect to the seasonal runoff climatology in Europe. *Water Resources Research*, 48(11).
- 651 Gudmundsson, L., Tallaksen, L. M., Stahl, K., Clark, D. B., Du-mont, E., Hagemann, S., Bertrand, N., Gerten, D., Heinke,
652 J., Hanasaki, N., Voss, F., and Koirala, S. (2012b). Comparing Large-Scale Hydrological Model Simulations to
653 Observed Runoff Percentiles in Europe, *J. Hydrometeorol.*, 13, 604–62.
- 654 Gupta VK, Waymire E, Wang CT. (1980). A representation of an instantaneous unit hydrograph from geomorphology.
655 *Water Resources Research* 16: 855–862, doi: 10.1029/WR016i005p00855.
- 656 Gupta, H. V., Kling, H., Yilmaz, K. K., & Martinez, G. F. (2009). Decomposition of the mean squared error and NSE
657 performance criteria: Implications for improving hydrological modelling. *Journal of Hydrology*, 377(1-2), 80-91.
- 658 Haddeland, I., Heinke, J., Voß, F., Eisner, S., Chen, C., Hagemann, S., & Ludwig, F. (2012). Effects of climate model
659 radiation, humidity and wind estimates on hydrological simulations. *Hydrology and Earth System Sciences*, 16(2),
660 305-318.
- 661 Hastie, T., Tibshirani, R., and Friedman, J. H. (2009). *The Elements of Statistical Learning – Data Mining, Inference, and*
662 *Prediction*, Second Edition, Springer Series in Statistics, Springer, New York, 2nd Edn., available at: [http://www-](http://www-stat.stanford.edu/~tibs/ElemStatLearn/)
663 [stat.stanford.edu/~tibs/ElemStatLearn/](http://www-stat.stanford.edu/~tibs/ElemStatLearn/) (last access: 5 July 2016).
- 664 Hong, Y., Adler, R. F., Hossain, F., Curtis, S., & Huffman, G. J. (2007). A first approach to global runoff simulation
665 using satellite rainfall estimation. *Water Resources Research*, 43(8).
- 666 Houborg, R., Rodell, M., Li, B., Reichle, R., & Zaitchik, B. F. (2012). Drought indicators based on model-assimilated
667 Gravity Recovery and Climate Experiment (GRACE) terrestrial water storage observations. *Water Resources*
668 *Research*, 48(7).
- 669 Hu GR., Li XY. (2018). Subsurface Flow. In: Li X., Vereecken H. (eds) *Observation and Measurement. Ecohydrology.*
670 Springer, Berlin, Heidelberg. https://doi.org/10.1007/978-3-662-47871-4_9-1
- 671 Huffman, G. J., R. F. Adler, D. T. Bolvin, G. J. Gu, E. J. Nelkin, K. P. Bowman, Y. Hong, E. F. Stocker, and D. B. Wolff.
672 (2007). The TRMM Multisatellite Precipitation Analysis (TMPA): Quasi-Global, Multiyear, Combined-Sensor
673 Precipitation Estimates at Fine Scales. *Journal of Hydrometeorology* 8 (1): 38–55. doi:10.1175/jhm560.1.
- 674 Huffman, G. J., Stocker, E. F., Bolvin, D. T., Nelkin, E. J., & Adler, R. F. (2014). TRMM Version 7 3B42 and 3B43 Data
675 Sets. NASA/GSFC, Greenbelt, MD.



- 676 Kim, H., Watanabe, S., Chang, E. C., Yoshimura, K., Hirabayashi, J., Famiglietti, J., and Oki, T. (2017). Global Soil
677 Wetness Project Phase 3 Atmospheric Boundary Conditions (Experiment 1) [Data set], Data Integration and Analysis
678 System (DIAS), <https://doi.org/10.20783/DIAS.501>.
- 679 Kirchner, J. W. (2006). Getting the right answers for the right reasons: Linking measurements, analyses, and models to
680 advance the science of hydrology. *Water Resources Research*, 42(3).
- 681 Kling, H., Fuchs, M., & Paulin, M. (2012). Runoff conditions in the upper Danube basin under an ensemble of climate
682 change scenarios. *Journal of Hydrology*, 424, 264-277, doi: 10.1016/j.jhydrol.2012.01.011.
- 683 Landerer, F. W., & Swenson, S. C. (2012). Accuracy of scaled GRACE terrestrial water storage estimates. *Water
684 resources research*, 48(4).
- 685 Lehner, B., C. Reidy Liermann, C. Revenga, C. Vörösmarty, B. Fekete, P. Crouzet, P. Döll, M. Endejan, K. Frenken, J.
686 Magome, C. Nilsson, J.C. Robertson, R. Rodel, N. Sindorf, and D. Wisser. 2011. High-resolution mapping of the
687 world's reservoirs and dams for sustainable river-flow management. *Frontiers in Ecology and the Environment* 9 (9):
688 494-502.
- 689 Long, D., Longuevergne, L., & Scanlon, B. R. (2014). Uncertainty in evapotranspiration from land surface modeling,
690 remote sensing, and GRACE satellites. *Water Resources Research*, 50(2), 1131-1151.
- 691 Lorenz, C., H. Kunstmann, B. Devaraju, M. J. Tourian, N. Sneeuw, and J. Riegger (2014). Large-Scale Runoff from
692 Landmasses: A Global Assessment of the Closure of the Hydrological and Atmospheric Water Balances. *J.
693 Hydrometeor.*, 15, 2111–2139, doi:10.1175/JHM-D-13-0157.1.
- 694 Luthcke, S.B., Sabaka, T.J., Loomis, B.D., Arendt, A.A., McCarthy, J.J., Camp, J. (2013) Antarctica, Greenland and Gulf
695 of Alaska land-ice evolution from an iterated GRACE global mascon solution, *Journal of Glaciology*, Vol. 59, No.
696 216, 2013 doi:10.3189/2013JoG12J147.
- 697 Massari, C., Brocca, L., Tarpanelli, A., Hong, Y., Crow, W., Ciabatta, L., Camici, S., Barbetta, S., Moramarco, T. (2016).
698 Global surface runoff estimation in near real time by using SMAP and GPM, poster at SMAP conference.
- 699 Massari, C., Brocca, L., Barbetta, S., Papanastasiou, C., Mimikou, M., & Moramarco, T. (2014). Using globally available
700 soil moisture indicators for flood modelling in Mediterranean catchments. *Hydrology and Earth System Sciences*,
701 18(2), 839.
- 702 Merz, R., & Blöschl, G. (2009). A regional analysis of event runoff coefficients with respect to climate and catchment
703 characteristics in Austria. *Water Resources Research*, 45(1).
- 704 Mueller Schmied, H., Adam, L., Eisner, S., Fink, G., Flörke, M., Kim, H., ... & Song, Q. (2016). Variations of global and
705 continental water balance components as impacted by climate forcing uncertainty and human water use. *Hydrology
706 and Earth System Sciences*, 20(7), 2877-2898.
- 707 Munepeerakul, R., Azalee, S., Botter, G., Rinaldo, A., & Rodriguez-Iturbe, I. (2010). Daily streamflow analysis based
708 on a two-scaled gamma pulse model. *Water Resources Research*, 46(11).
- 709 Nash, J. E. (1957). The form of the instantaneous unit hydrograph, IASH publication no. 45, 3–4, 114–121.
- 710 Natural Resources Conservation Service (NRCS) (1986), Urban hydrology for small watersheds, Tech. Release 55, 2nd
711 ed., U.S. Dep. of Agric., Washington, D. C. (available at [ftp://ftp.wcc.nrcs.usda.gov/downloads/
712 hydrology_hydraulics/tr55/tr55.pdf](ftp://ftp.wcc.nrcs.usda.gov/downloads/hydrology_hydraulics/tr55/tr55.pdf))
- 713 Orth, R., & Seneviratne, S. I. (2015). Introduction of a simple-model-based land surface dataset for Europe.
714 *Environmental Research Letters*, 10(4), 044012.
- 715 Pellet, V., Aires, F., Munier, S., Fernández Prieto, D., Jordá, G., Dorigo, W. A., ... & Brocca, L. (2019). Integrating
716 multiple satellite observations into a coherent dataset to monitor the full water cycle—application to the Mediterranean
717 region. *Hydrology and Earth System Sciences*, 23(1), 465-491.
- 718 Prudhomme, C., Giuntoli, I., Robinson, E. L., Clark, D. B., Arnell, N. W., Dankers, R., ... & Hagemann, S. (2014).
719 Hydrological droughts in the 21st century, hotspots and uncertainties from a global multimodel ensemble experiment.
720 *Proceedings of the National Academy of Sciences*, 111(9), 3262-3267.
- 721 Rakovec, O., Kumar, R., Attinger, S., & Samaniego, L. (2016). Improving the realism of hydrologic model functioning
722 through multivariate parameter estimation. *Water Resources Research*, 52(10), 7779-7792.



- 723 Richards, L.A. (1931). Capillary conduction of liquids through porous mediums. *Physics*. 1 (5): 318–333.
724 Bibcode:1931Physi.1.318R. doi:10.1063/1.1745010.
- 725 Riegger, J., and M. J. Tourian (2014), Characterization of runoff-storage relationships by satellite gravimetry and remote
726 sensing, *Water Resour. Res.*, 50, 3444–3466, doi:10.1002/2013WR013847.
- 727 Rodell, M., Beaudoin, H. K., L’Ecuyer, T. S., Olson, W. S., Famiglietti, J. S., Houser, P. R., Adler, R., Bosilovich, M.
728 G., Clayson, C. A., Chambers, D., Clark, E., Fetzer, E. J., Gao, X., Gu, G., Hilburn, K., Huffman, G. J., Lettenmaier,
729 D. P., Liu, W. T., Robertson, F. R., Schlosser, C. A., Sheffield, J. and Wood, E. F. (2015). The observed state of the
730 water cycle in the early 15twenty-first century, *J. Clim.*, 28(21), 8289–8318, doi:10.1175/JCLI-D-14-00555.1.
- 731 Schellekens, J., Dutra, E., Martínez-de la Torre, A., Balsamo, G., van Dijk, A., Sperna Weiland, F., Minvielle, M., Cal-
732 vet, J.-C., Decharme, B., Eisner, S., Fink, G., Flörke, M., Peßenteiner, S., van Beek, R., Polcher, J., Beck, H., Orth, R.,
733 Calton, B., Burke, S., Dorigo, W., and Weedon, G. P. (2017). A global water resources ensemble of hydrological
734 models: the earth2Observe Tier-1 dataset, *Earth Syst. Sci. Data*, 9, 389–413, <https://doi.org/10.5194/essd-9-389-2017>.
- 735 Schwanghart, W., & Kuhn, N. J. (2010). TopoToolbox: A set of Matlab functions for topographic analysis. *Environmental*
736 *Modelling & Software*, 25(6), 770–781.
- 737 Seneviratne, S. I., Corti, T., Davin, E. L., Hirschi, M., Jaeger, E. B., Lehner, I., ... & Teuling, A. J. (2010). Investigating
738 soil moisture–climate interactions in a changing climate: A review. *Earth-Science Reviews*, 99(3–4), 125–161.
- 739 Sneeuw, N., Lorenz, C., Devaraju, B., Tourian, M. J., Riegger, J., Kunstmann, H., & Bárdossy, A. (2014). Estimating
740 runoff using hydro-geodetic approaches. *Surveys in Geophysics*, 35(6), 1333–1359.
- 741 Solomatine, D. P., & Ostfeld, A. (2008). Data-driven modelling: some past experiences and new approaches. *Journal of*
742 *hydroinformatics*, 10(1), 3–22.
- 743 Tapley, B.D., Watkins, M.M., Flechtner, F. et al. (2019). Contributions of GRACE to understanding climate change. *Nat.*
744 *Clim. Chang.* 9, 358–369, doi:10.1038/s41558-019-0456-2.
- 745 Thiemeig, V., Rojas, R., Zambrano-Bigiarini, M., & De Roo, A. (2013). Hydrological evaluation of satellite rainfall
746 estimates over the Volta and Baro-Akobo Basin. *Journal of Hydrology*, 499, 324–338.
- 747 Tourian, M. J., Reager, J. T., & Sneeuw, N. (2018). The total drainable water storage of the Amazon river basin: A first
748 estimate using GRACE. *Water Resources Research*, 54. <https://doi.org/10.1029/2017WR021674>.
- 749 Trambly, Y., Bouvier, C., Martin, C., Didon-Lescot, J. F., Todorovik, D., & Domergue, J. M. (2010). Assessment of
750 initial soil moisture conditions for event-based rainfall–runoff modelling. *Journal of Hydrology*, 387(3–4), 176–187.
- 751 Troutman, B. M., Karlinger, M.B. (1985). Unit hydrograph approximation assuming linear flow through topologically
752 random channel networks. *Water Resources Research*, 21: 743 – 754, doi: 10.1029/WR021i005p00743.
- 753 Vose, R.S., Applequist, S., Durre, I., Menne, M.J., Williams, C.N., Fenimore, C., Gleason, K., & Arndt, D. (2014).
754 Improved Historical Temperature and Precipitation on Time Series For U.S. Climate Divisions. *Journal of Applied*
755 *Meteorology and Climatology*, 53(May), 1232–1251. DOI: 10.1175/JAMC-D-13-0248.1
- 756 Vörösmarty C. J., and Coauthors (2002). Global water data: A newly endangered species. *Eos, Trans. Amer. Geophys.*
757 *Union*, 82, 54.
- 758 Wagner, W., Blöschl, G., Pampaloni, P., Calvet, J. C., Bizzarri, B., Wigneron, J. P., & Kerr, Y. (2007). Operational
759 readiness of microwave remote sensing of soil moisture for hydrologic applications. *Hydrology Research*, 38(1), 1–
760 20.
- 761 Wagner, W., Lemoine, G., & Rott, H. (1999). A method for estimating soil moisture from ERS scatterometer and soil
762 data. *Remote Sensing of Environment*, 70, 191–207, doi:10.1016/S0034-4257(99)00036-X.
- 763 Wissler, D., Fekete, B. M., Vörösmarty, C. J., and Schumann, A. H. (2010). Reconstructing 20th century global
764 hydrography: a contribution to the Global Terrestrial Network- Hydrology (GTN-H), *Hydrological Earth Syst. Sci.*, 14, 1–
765 24, doi:10.5194/hess-14-1-2010.
- 766 Yokoo, Y., & Sivapalan, M. (2011). Towards reconstruction of the flow duration curve: Development of a conceptual
767 framework with a physical basis. *Hydrology and Earth System Sciences*, 15(9), 2805–2819.
768 <https://doi.org/10.5194/hess-15-2805-2011>.



769 Zhang, Y., Pan, M., Sheffield, J., Siemann, A. L., Fisher, C. K., Liang, M., ... & Zhou, T. (2018). A Climate Data Record
770 (CDR) for the global terrestrial water budget: 1984–2010. Hydrology and Earth System Sciences (Online), 22(PNNL-
771 SA-129750).
772



773 Table 1. Location of gauging stations over the Mississippi basins and upstream contributing area. Red
 774 colored text indicates stations where the STREAM model has been calibrated.

#	River	Station name	Latitude (°)	Longitude (°)	Upstream area (km ²)	Mean annual river discharge (m ³ /s)	Presence of dam
1	Missouri	Bismarck, ND	-100.82	46.81	481'232	633	Garrison dam
2	Missouri	Omaha, NE	-95.92	41.26	814'371	914	Gavins Point Dam
3	Missouri	Kansas City, MO	-94.59	39.11	1'229'427	1499	---
4	Missouri	Hermann, MO	-91.44	38.71	1'330'000	2326	---
5	Kansas	Wamego, KS	-96.30	39.20	143'054	141	Kanopolis
6	Mississippi	Keokuk, IA	-91.37	40.39	282'559	1948	---
7	Rock	Near Joslin, IL	-90.18	41.56	23'835	199	---
8	Mississippi	Chester, IL	-89.84	37.90	1'776'221	6018	---
9	Arkansas	Murray Dam Near Little Rock, AR	-92.36	34.79	408'068	1249	---
10	Mississippi	Vicksburg, MS	-90.91	32.32	2'866'590	17487	---
11	Ohio	Metropolis, ILL.	-88.74	37.15	496'134	7931	---

775
 776

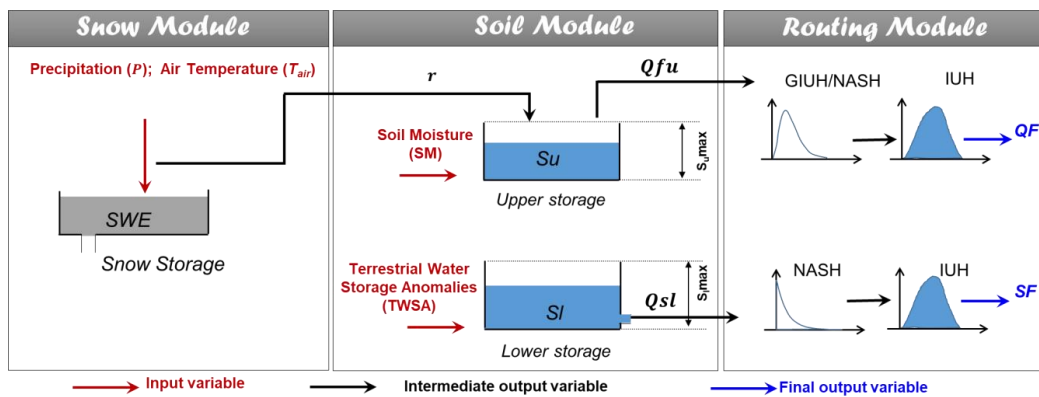
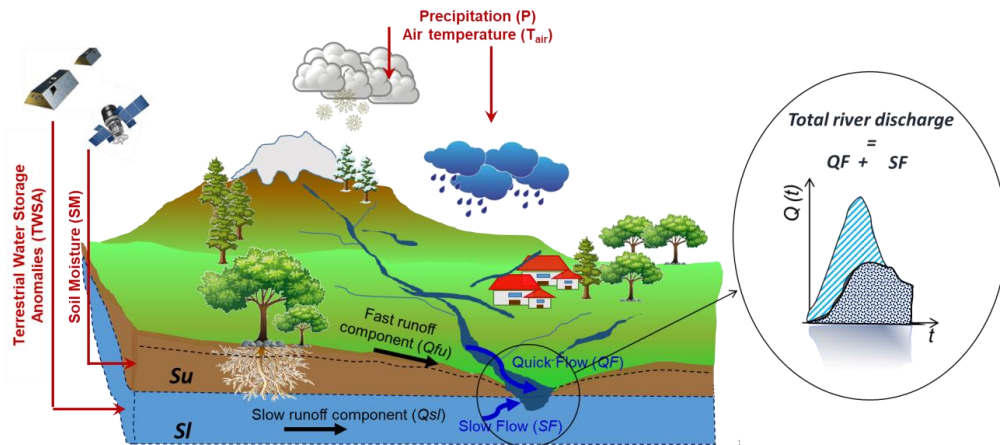


777 Table 2. Performance scores obtained over the Mississippi river sections during the calibration and
 778 validation periods.

#	CALIBRATION PERIOD			VALIDATION PERIOD		
SCORE	KGE (-)	R (-)	RRMSE (%)	KGE (-)	R (-)	RRMSE (%)
CALIBRATED SECTIONS						
10	0.78	0.78	30	0.74	0.80	38
9	0.62	0.75	71	0.67	0.85	77
6	0.83	0.84	39	0.73	0.84	46
4	0.77	0.78	46	0.72	0.75	50
11	0.82	0.82	44	0.70	0.86	51
SECTIONS NOT USED FOR CALIBRATION						
1	-3.26	0.08	137	0.20	0.44	96
2	-0.57	0.48	118	0.40	0.53	89
3	0.16	0.71	83	0.39	0.70	72
5	-1.49	0.24	368	-1.26	0.31	358
7	0.53	0.68	71	0.20	0.70	81
8	0.80	0.84	36	0.77	0.84	39

779

780



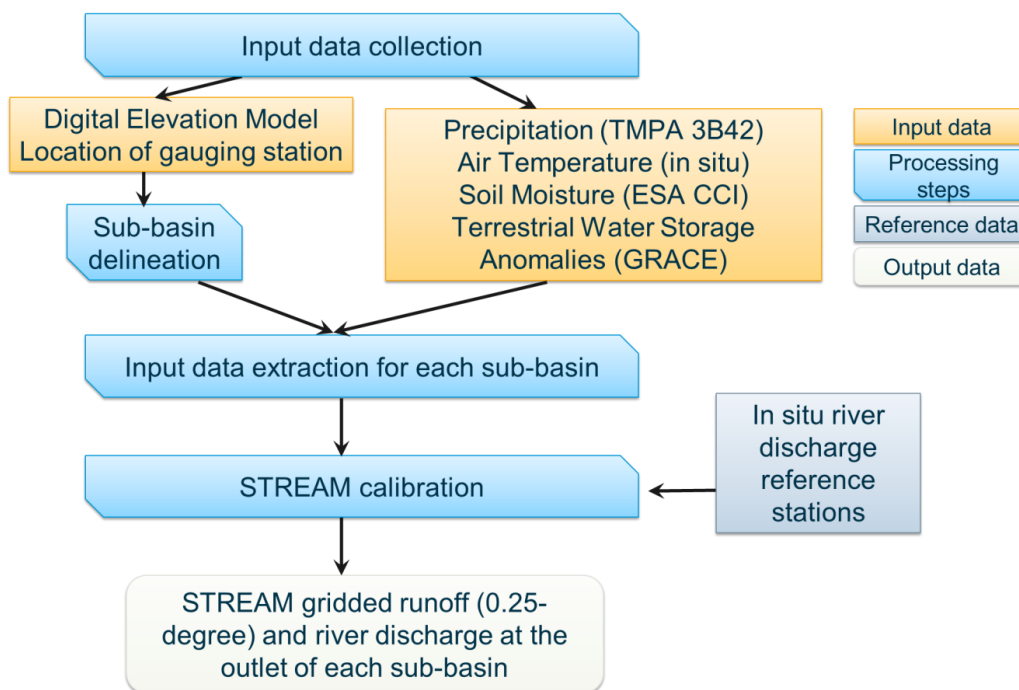
781

782 Figure 1. Configuration of the STREAM model adopted for total runoff estimation. The model
 783 includes three modules, the snow module allowing to separate snowfall from rainfall, the soil module
 784 that simulates the slow and quick runoff components (Q_{su} and Q_{fu} , respectively) and the routing
 785 module for flood simulation. Red arrows indicate input variables; black arrows indicate intermediate
 786 output variables; blue arrows indicate final output variables. The components Q_{fu} and Q_{su}
 787 are computed by using satellite P , soil moisture and TWSA data as input to the soil module. Please refer
 788 to text for symbols.

789



790

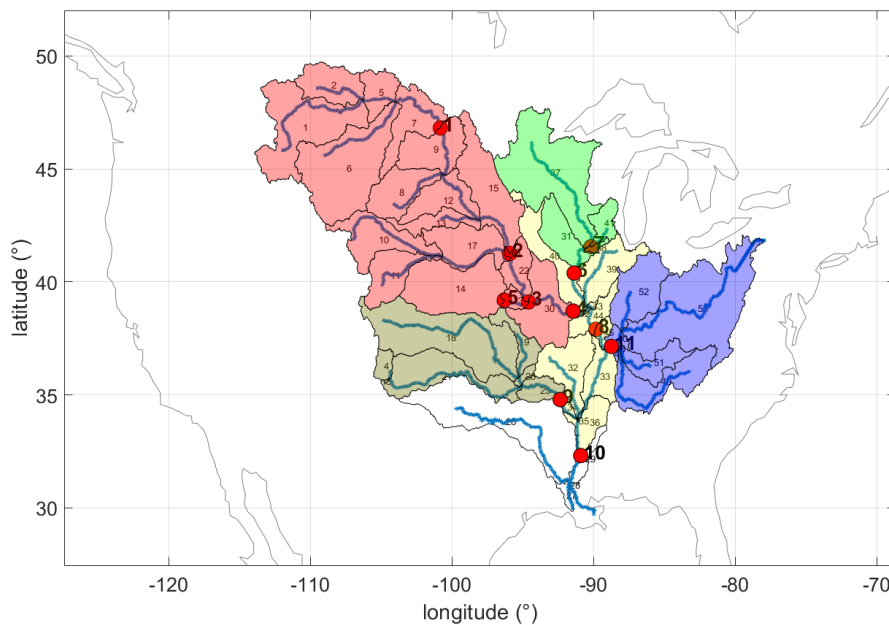


791
792
793
794

Figure 2. Processing steps of the STREAM approach.



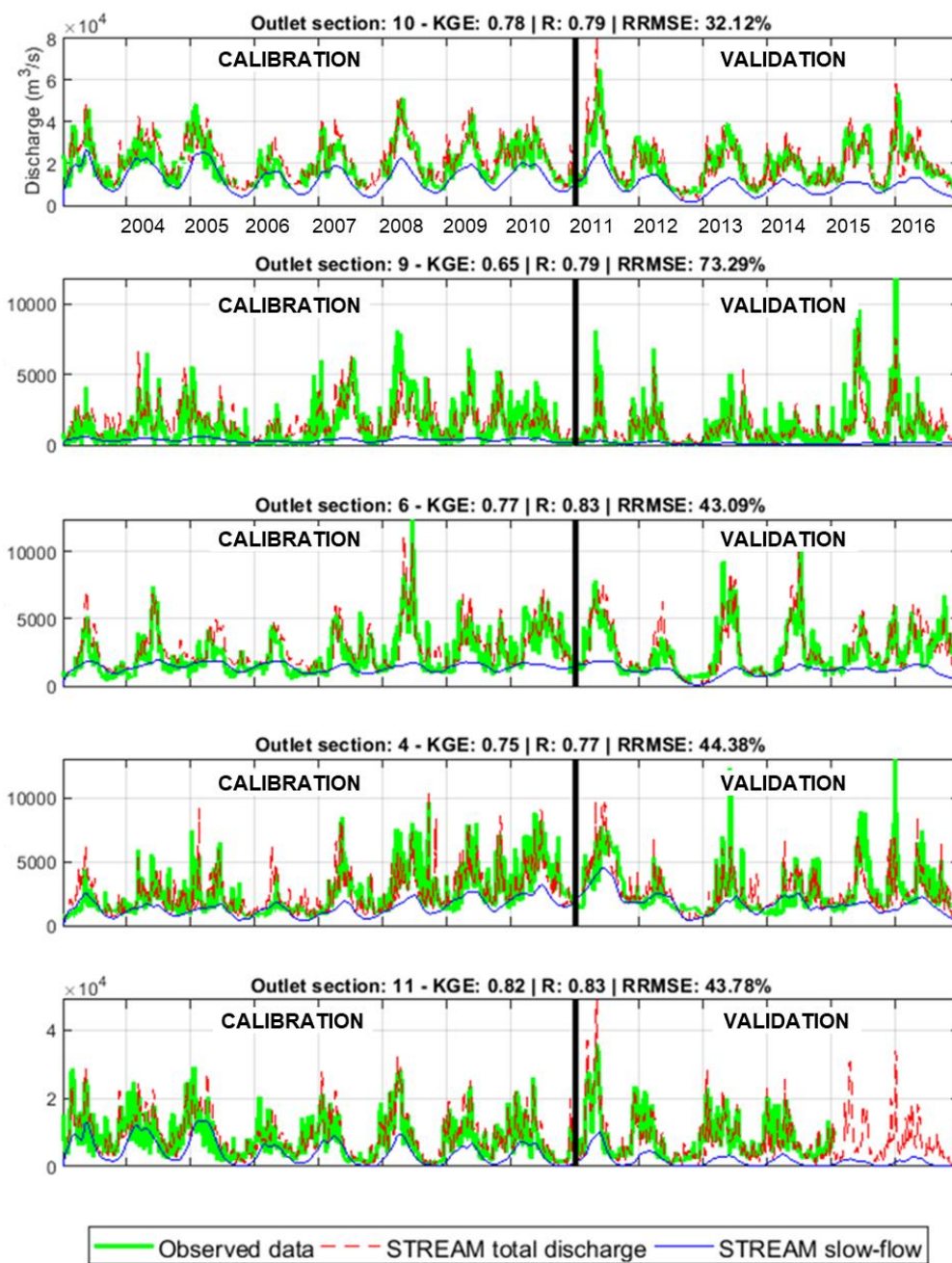
795



796

797 Figure 3. Mississippi sub-basin delineation. Red dots indicate the location of the discharge gauging
798 stations; different colours identify different inner sections (and the related contributing sub-basins)
799 used for the model calibration.

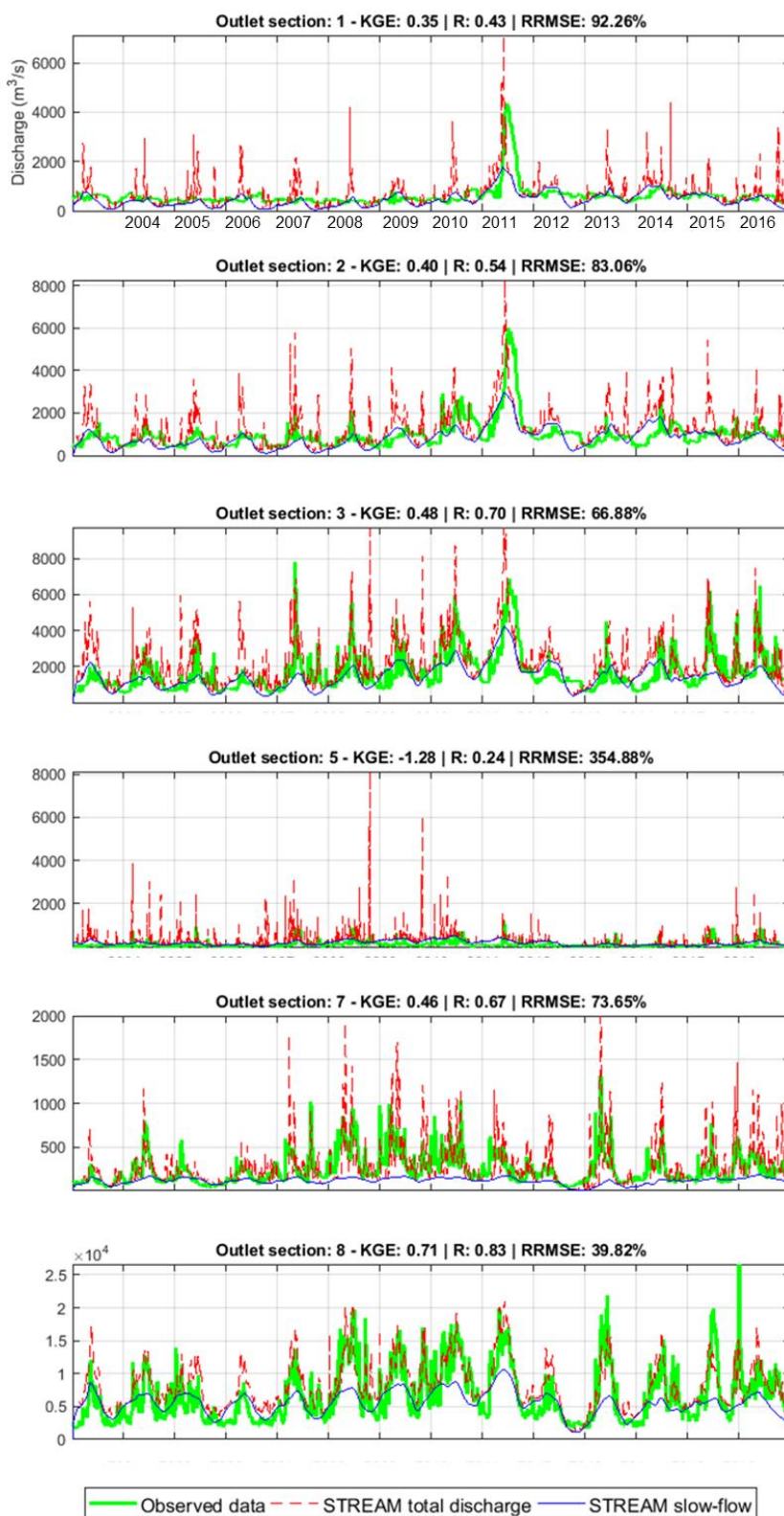
800



801

802 Figure 4. Comparison between observed and simulated river discharge time series over the five
803 calibrated sections over Mississippi river basin. Performance scores at the top of each plot refer to
804 the entire study period (2003–2016).

805

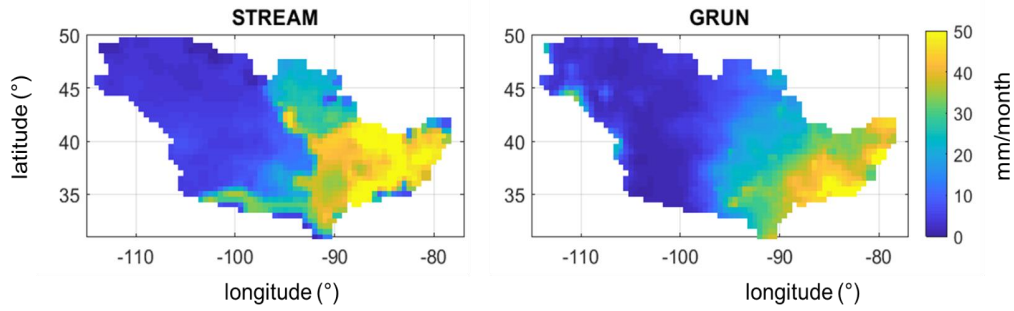




808

809 Figure 5. Comparison between observed and simulated river discharge time series over the gauged
810 sections not used in the calibration phase. Performance scores at the top of each plot refer to the entire
811 study period (2003–2016).

812



813

814 Figure 6. Mississippi river basin: mean monthly runoff for the period 2003–2014 obtained by
815 STREAM and GRUN models.